forests

MDPI

Article

Classification and Observed Seasonal Phenology of Broadleaf Deciduous Forests in a Tropical Region by Using Multitemporal Sentinel-1A and Landsat 8 Data

Anh Tuan Tran [1], Kim Anh Nguyen [2,3,*], Yuei An Liou [2,*], Minh Hang Le [4], Van Truong Vu [4] and Dinh Duong Nguyen [3]

[1] Institute of Ecology and Biological Resources, Vietnam Academy of Science and Technology, 18 Hoang Quoc Viet Rd., Cau Giay Dist., Hanoi City 100 000, Vietnam; tuan.ig@gmail.com
[2] Center for Space and Remote Sensing Research, National Central University, No. 300, Zhongda Rd., Zhongli Dist., Taoyuan City 320317, Taiwan
[3] Institute of Geography, Vietnam Academy of Science and Technology, 18 Hoang Quoc Viet Rd., Cau Giay Dist., Hanoi City 100 000, Vietnam; duong.nguyen2007@gmail.com
[4] Institute of Techniques for Special Engineering (ITSE), Le Quy Don Technical University, No. 236 Hoang Quoc Viet Rd., Bac Tu Liem Dist., Hanoi City 100 000, Vietnam; leminhhang81@gmail.com (M.H.L.); Truongvv@lqdtu.edu.vn (V.T.V.)
* Correspondence: nguyenrose@csrsr.ncu.edu.tw (K.A.N.); yueian@csrsr.ncu.edu.tw (Y.A.L.); Tel.: +886-3-4227151 (ext. 57631) (K.A.N.)

Citation: Tran, A.T.; Nguyen, K.A.; Liou, Y.A.; Le, M.H.; Vu, V.T.; Nguyen, D.D. Classification and Observed Seasonal Phenology of Broadleaf Deciduous Forests in a Tropical Region by Using Multitemporal Sentinel-1A and Landsat 8 Data. *Forests* **2021**, *12*, 235. https://doi.org/10.3390/f12020235

Academic Editors: Sofia Bajocco and Panayotis Dimopoulos

Received: 8 December 2020
Accepted: 15 February 2021
Published: 18 February 2021

Abstract: Broadleaf deciduous forests (BDFs) or dry dipterocarp forests play an important role in biodiversity conservation in tropical regions. Observations and classification of forest phenology provide valuable inputs for ecosystem models regarding its responses to climate change to assist forest management. Remotely sensed observations are often used to derive the parameters corresponding to seasonal vegetation dynamics. Data acquired from the Sentinel-1A satellite holds a great potential to improve forest type classification at a medium-large scale. This article presents an integrated object-based classification method by using Sentinel-1A and Landsat 8 OLI data acquired during different phenological periods (rainy and dry seasons). The deciduous forest and nondeciduous forest areas are classified by using NDVI (normalized difference vegetation index) from Landsat 8 cloud-free composite images taken during dry (from February to April) and rainy (from June to October) seasons. *Shorea siamensis* Miq. (*S. siamensis*), *Shorea obtusa* Wall. ex Blume (*S. obtusa*), and *Dipterocarpus tuberculatus* Roxb. (*D. tuberculatus*) in the deciduous forest area are classified based on the correlation between phenology of BDFs in Yok Don National Park and backscatter values of time-series Sentinel-1A imagery in deciduous forest areas. One hundred and five plots were selected during the field survey in the study area, consisting of dominant deciduous species, tree height, and canopy diameter. Thirty-nine plots were used for training to decide the broadleaf deciduous forest areas of the classified BDFs by the proposed method, and the other sixty-six plots were used for validation. Our proposed approach used the changes of backscatter in multitemporal SAR images to implement BDF classification mapping with acceptable accuracy. The overall accuracy of classification is about 79%, with a kappa coefficient of 0.7. Accurate classification and mapping of the BDFs using the proposed method can help authorities implement forest management in the future.

Keywords: broadleaf deciduous forests; forest classification; sentinel; Landsat; multiresolution segmentation algorithm

1. Introduction

Dry dipterocarp forest (DDF) or broadleaf deciduous forest (BDF) is a typical forest of Southeast Asian countries dominated by humid tropical climate with a rainy and a severe dry season. Generally speaking, BDFs are distributed in Laos, Cambodia, Thailand,

Indonesia, Malaysia, Philippines, and some other South Asian countries. In Vietnam, BDFs are dominated by Dipterocarpaceae with deciduous season in the dry season. BDFs play an important role in the life of flora and fauna in the Central Highlands, Vietnam. In recent years, BDFs have been gradually replaced by industrial trees that are expected to generate higher economic values [1]. Nevertheless, it has been found that both natural and human-made disturbances could deteriorate the ecosystems. For instance, it has been found that Asia's ecoenvironment is very vulnerable to massive changes in the land use and land cover [2]. It is thus suggested that environmental protection is crucial by controlling the access to forestry, limiting agricultural activities, and enhancing green industry to improve environmental facilities and restore ecological values [3]. Evidently, observation and classification of forest phenology provide valuable information for the improved forest management to achieve environmental sustainability. Forest phenology is the first-order control on terrestrial carbon and energy budgets, while Earth observations are usually utilized to derive parameters of the seasonal vegetation dynamics in ecosystem models.

Vegetation phenology is defined as the study of a plant's life cycles influenced by the environmental seasonality [4]. The long-term in situ observations have been used to demonstrate the plant phenology at the species level [5], while satellite-based observations have been used to analyze ecosystems' leaf phenology at global scale [6]. For the long-term timespan over large-scale areas, Landsat time-series data and the Moderate Resolution Imaging Spectroradiometer (MODIS) are valuable sources of datasets to support forest mapping and studies [7–9]. At global scale, MODIS products were designed to consistently provide spatiotemporal global vegetation conditions to assist change detection and phenological and biophysical interpretations [10,11]. In contrast, at smaller scale, Landsat data are used for studying forest phenology. The Landsat satellite is an instrument for monitoring and identifying patterns of forest land cover and land use change. In the past, the use of Landsat data to derive forest information significantly contributed to the global system database for further investigating environmental issues [12–17]. Analysis of the plant phenology using remote sensing data is based on the seasonal trajectory of vegetation indices, such as the normalized difference vegetation index (NDVI) or enhanced vegetation index (EVI) [18–22]. Moreover, the timing of phenological transition was determined by the vegetation index threshold [23,24].

Many studies have been proposed to discriminate tree species and crops based on multitemporal optical data [25,26], hyperspectral data [27,28], and radar data [29,30]. The information of the species is mainly extracted based on the correlation between the phenology of plants and spectral reflection or backscatter signal in satellite images. The multitemporal Sentinel-1A data have been useful in monitoring phenology and classifying deciduous forests [29,31]. Marius et al. [29] utilized multitemporal Sentinel-1A to monitor phenology and classify two forest types as deciduous and coniferous forests in northern Switzerland with classification accuracy of 86%. To improve accuracy, simultaneous use of optical and radar images, either multitemporal optical images or a single SAR image [32], or multitemporal SAR images and a single optical image [33], is adopted. Using Advanced Land Observation Satellite (ALOS) Phased Array type L-band Synthetic Aperture Radar (PALSAR) combined with Sentinel-2A data to determine forest cover and biomass variation has been presented in the literature [34–36]. The classification methods as pixel-based and object-based methods were used for vegetation species classification [25,28,29,37]. An object-based method is applied for image classification or land cover and forest mapping using a time series of satellite images.

According to the Global Forest Report [38], Vietnam is one of the top leading countries in forest cover loss, although various forest protection and reforestation programs have been implemented. It is estimated that from 2001 to 2007, Vietnam lost 2.42 Mha of tree cover, equivalent to a 15% decrease since 2000 and 256 Mha of CO_2 emissions [38]. Therefore, there is a need to have a better forest management solution with detailed observation of forest tree species to assist forest officials and local authorities in advancing forest management and restoration.

This research proposes an object-based classification method to identify BDFs by integrating multitemporal Sentinel-1A images with a spatial resolution of 10 m and Landsat 8 OLI images with a spatial resolution of 30 m. Yok Don National Park, located in Central Highlands, Vietnam, is selected as the study site. Since it is characterized by a rich ecosystem of dry open dipterocarp forest mixed with broadleaved tropical evergreen forests with high plant diversity in high mountainous areas, the intersection and mixing of diverse forest species result in challenges for forest monitoring and management. It is the first time the integration of multitemporal Sentinel-1A and Landsat images is adopted to identify dominant deciduous forest species in the Central Highlands and tropical region based on the correlation between backscatter values of multitemporal Sentinel-1A images and the phenological difference in leaf regeneration periods of dipterocarp trees. The outcomes of this study will contribute to further applications of combining freely accessible optical and radar satellite images in studying forest tree species in tropical regions.

2. Study Site

Yok Don National Park is one of the largest protected areas, situated in the Dak Lak and Dak Nong provinces, Central Highlands, Vietnam. It lies between latitudes 12°45′ and 13°10′ N, and longitudes 107°29′30′′ and 107°48′30′′ E (Figure 1).

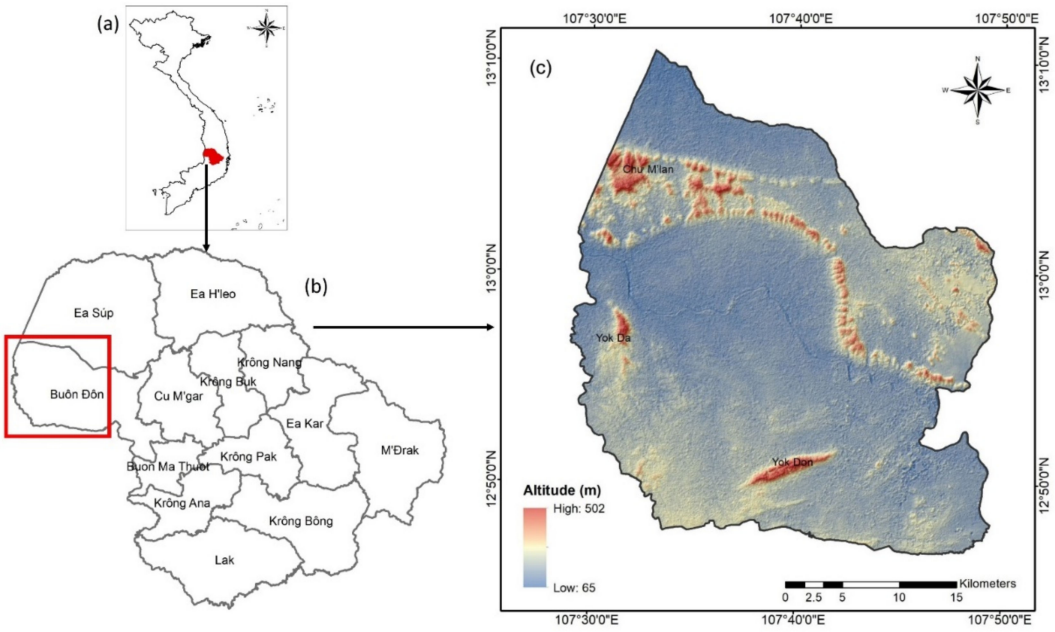

Figure 1. The study area in Yok Don National Park, Dak Lak Province, in the Central Highlands of Vietnam. (**a**) Vietnam administrative boundary; (**b**) administrative boundary of Dak Lak Province at district level and the study area located in red rectangle; and (**c**) topography of Yok Don National Park.

The total area is 115,545 ha, divided into three zones, including strict protection zone of 80,947 ha, ecological restoration zone of 30,426 ha, and administrative service zone of 4172 ha. The buffer zone covers an area of 133,890 ha, including the communes surrounding the national park. The terrain is relatively flat with an average elevation of about 200 m above sea level. In the study area, there are three peaks, including Chư M'lan (502 m), Yok Don (482 m), and Yok Da (466 m) mountains (Figure 1). The average annual rainfall of the study area is less than 1600 mm. The climate in Yok Don is divided into two seasons, i.e., the rainy season from May to October and the dry season from November to April. The annual average temperature is about 24.5 °C with the highest temperature of the year about 37.5 °C and the lowest temperature at about 11 °C. The highest average temperature occurs typically in April and the lowest average temperature usually appears in January.

Yok Don National Park was selected as a test site with typical and conserved BDFs. Primary forest accounts for over 90% of the total area of the park, an ideal habitat for plant and animal species. Especially, Yok Don is the only area in Vietnam that preserves the forest type of dipterocarp forest (http://yokdonnationalpark.vn). BDFs have large valuable timber species and nontimber forest products, such as oil and medicinal herbs, and they are habitats for animal groups. They play a crucial role in the livelihoods of many local ethnic minority communities. Yok Don National Park is one of the places to preserve the biodiversity of deciduous forests so that dominant species are relatively homogeneous and less affected by human activities and ecological succession, mainly based on natural habitats. Hence, it is a good site for testing multitemporal remote sensing data for studying the deciduous forest.

The vegetation within Yok Don National Park is mainly a combination of BDFs, semi-evergreen forests with a smaller evergreen forest area, which grows mainly on hills and along with watercourses. The BDFs primarily consist of members of the family Dipterocarpaceae, including *Dipterocarpus tuberculatus*, *Shorea siamensis*, *Shorea obtuse*, and *Dipterocarpus obtusifolius* Teijsm. ex Miq. [39].

3. Materials and Methods

3.1. Satellite Data and Image Preprocessing

Due to the climatic and topographical features of Yok Don in the rainy season, clouds often occur and cause difficulties in obtaining cloudless images. Hence, we collected six scenes of Landsat 8 images in the dry season during the timeframe from January to March 2015 and 12 scenes of Landsat 8 images in the rainy season from June to October 2015 and from June to August 2016, as shown in Table 1, to create a Landsat 8 cloud-free composite image for each season. The Yok Don National Park's forest status was unchanged during 2015–2016 since it is strictly protected and forests have steadily grown.

Table 1. Landsat 8 images used in this study.

Specifications	Landsat 8/T1_TOA
Acquisition time	
In dry season (6 scenes)	01 January 2015; 17 January 2015; 02 February 2015; 18 February 2015; 06 March 2015; 22 March 2015
In rainy season (12 scenes)	10 June 2015; 26 June 2015; 12 July 2015; 28 July 2015; 13 August 2015; 29 August 2015; 30 September 2015; 16 October 2015; 12 June 2016; 14 July 2016; 30 July 2016; 15 August 2016
Path/Row	124/51
Level	Level-1
Band	Blue, Green, Red, NIR, SWIR-1, and SWIR-2
Resolution	30 m
Bit depth	16 bits

The Landsat 8 images were preprocessed by using the Google Earth Engine (GEE) platform. The main processing steps include (i) acquisition of the surface reflectance product from the USGS, (ii) selection of the input target scene and reference scenes, (iii) detection of clouds and masking their shadow areas on the images, and (iv) replacing the cloud and cloud-shadow pixels on the target image with cloudless pixels from the reference image corresponding to their coordinates, which ensured that the output composite images were filled by cloud-free pixels to serve for image classification. Figure 2 shows the result of the output composite images (red = SWIR1 band, green = NIR band, blue = RED band) of Landsat 8 over the study area.

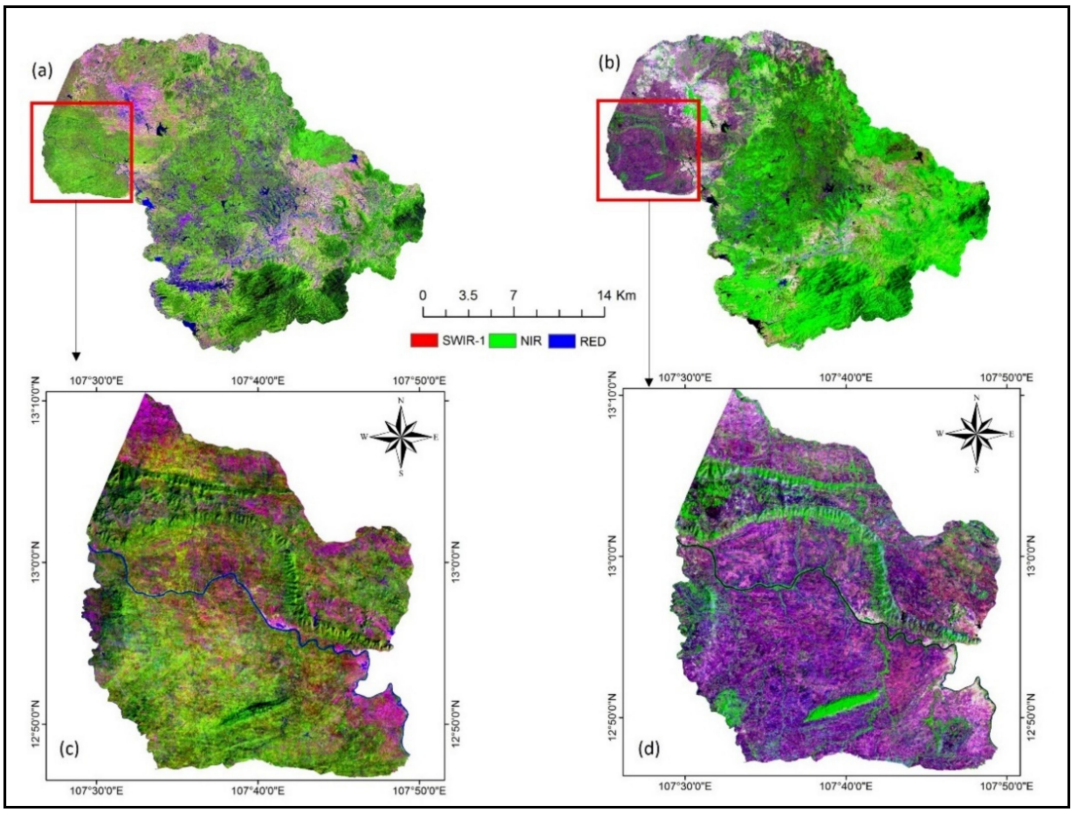

Figure 2. Landsat 8 cloud-free composite images in the rainy (**a**,**c**) and dry (**b**,**d**) seasons in Yok Don National Park.

Sentinel-1A provides active microwave data that are not affected by weather conditions, day and night. The repeat cycle of Sentinel-1A is 12 days. To classify the forest species, we selected nine scenes of Sentinel-1A monthly from February to December in 2015, as seen in Table 2.

Table 2. Multitemporal Sentinel-1A data used in this study.

Specifications	Sentinel-1A Data
Acquisition time	22 February 2015; 30 March 2015; 17 May 2015; 28 July 2015; 21 August 2015; 14 September 2015; 08 October 2015; 01 November 2015; 19 December 2015
Ascending/Descending	Ascending
Mode	IW (Interferometry Wide Mode)
Band	C-band (5.46 Hz)
Polarization	VV and VH
Level processing	Level-1 GRD (Ground Range Detected)
Resolution	10 × 10 m
Bit depth	16 bits

The Sentinel-1A dataset was used to classify deciduous forests based on differential backscatter values (dB) corresponding to the phenology of dominant deciduous species. Thus, it is necessary to have satellite images at the right time of the season to analyze seasonal variation of phenology and differences in forest species' leaf regeneration. Therefore, we selected multiple scenes and chose one scene for each month. However, Sentinel-1A data in Dak Lak Province, Vietnam, were missing for some months, namely January, April, and June.

The multitemporal Sentinel-1A images are preprocessed by the Sentinel Application Platform (SNAP) toolbox provided by the European Space Agency (ESA). The preprocessing consists of the following steps: (i) calibrating data to sigma naught value (σ^0), (ii)

performing terrain correction by using the Shuttle Radar Topography Mission (SRTM) Digital Elevation Model (DEM), (iii) performing dB value conversion, and (iv) implementing multitemporal speckle filtering. In order to integrate the data for further analysis, all the images need to be in the same resolution and projection, so that all images were setup in the the WGS-84 UTM Zone 49N projection, and the Landsat images were resampled to be 10 m resolution, the same as the resolution of Sentinel-1A data.

In general, the study area's terrain is relatively flat, so that we used the SRTM DEM with 30 m resolution for geometric distortion correction. It was found that only some hilly areas and mountains were affected by foreshortened slopes in the SAR image, which caused the brightness reflectance features on the image. Therefore, we had difficulties distinguishing the vegetation in the high mountains with Sentinel-1A. In contrast, the vegetation in the high mountains can be classified by using optical satellite images. We chose to classify the vegetation species in these mountainous regions by Landsat 8 OLI images to solve this difficulty.

3.2. Field Survey Data

The surveying data collected at Yok Don National Park, Dak Lak Province, in April 2015 in the dry season were used for finding the dominant species of broadleaf deciduous forest and validating the result. One hundred and five plots (12 plots of semi-evergreen/evergreen forest, 15 plots of *Shorea siamensis*, 36 plots of *Shorea obtusa*, and 42 plots of *Dipterocarpus tuberculatus*) were selected as shown in Figure 3. Among them, 39 plots (four plots of semi-evergreen forest, 8 plots of *S. siamensis*, 13 plots of *S. obtusa*, and 14 plots of *D. tuberculatus*) were used for training and 66 plots were used for validation of the classification result. Each plot size covers an area of 20 m × 20 m. In each sample plot, we collected parameters, including specimen, tree height, tree diameter at breast height, vegetation type, number of individuals and cover that represent the main dominant species (or broadleaf deciduous forest) plots, and their coordinates. The selected plots had to represent the main dominant species, spatial distribution, density, and structure. The distance between plots was usually chosen to be at least 200 m and the location at least 100 m close to the other dominant species.

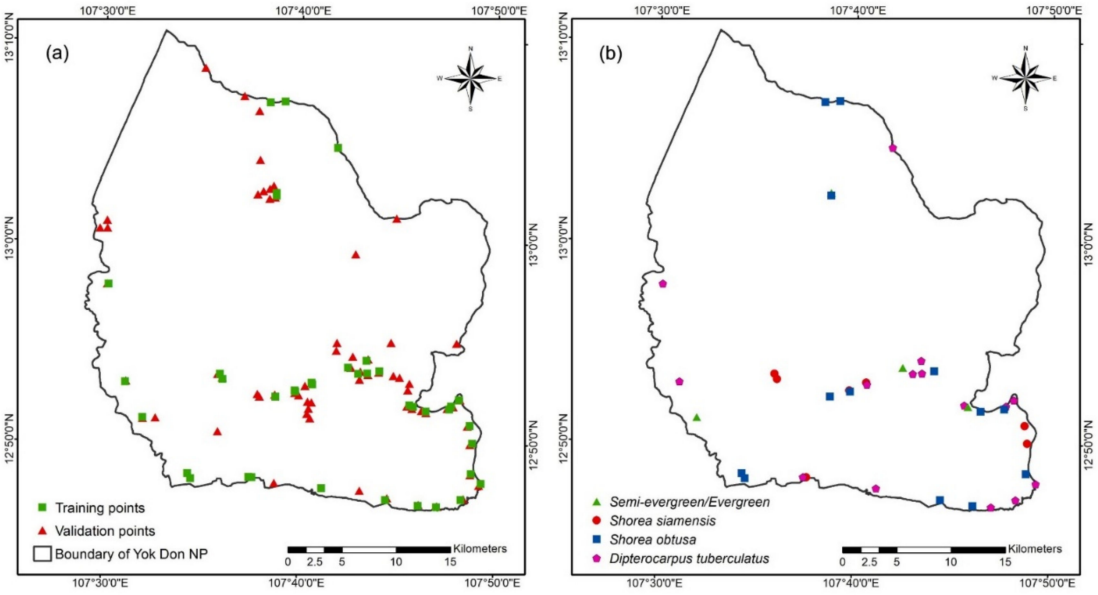

Figure 3. (**a**) Distribution of field survey data: (**a**) plots used for training are shown in green and plots used for validation are shown in red and (**b**) spatial distribution of the 39 field survey plots of the four types of deciduous forest used for training.

In order to determine certain forest states in which species are dominant in a plot, the basal area was applied for this study [40]. The basal area is one of the chief characteristics

determining dominance and nature of the community. It refers to the ground actually penetrated by the stems. Basal area can be measured through:

$$BA(\text{spm}) = \pi r^2 = \frac{3.1416 \times (\text{diameter})^2}{4} \quad (1)$$

$$RBA\ (\%) = \frac{\text{BA of individual species}}{\text{Total BA of all species}} \times 100 \quad (2)$$

where *BA* is basal area and *RBA* is relative basal area. Thus, in plots, the species with the largest *RBA* will be the dominant species.

3.3. Methodology

3.3.1. NDVI Images

NDVI images were generated from Landsat 8 cloud-free composite images for the dry and rainy seasons, as shown in Figure 4. The formula for determining NDVI is shown in Equation (3):

$$\text{NDVI} = \frac{(\text{NIR} - \text{RED})}{(\text{NIR} + \text{RED})} \quad (3)$$

where NIR is the surface reflectance value of the near-infrared band and RED is the surface reflectance value of the red band of Landsat images.

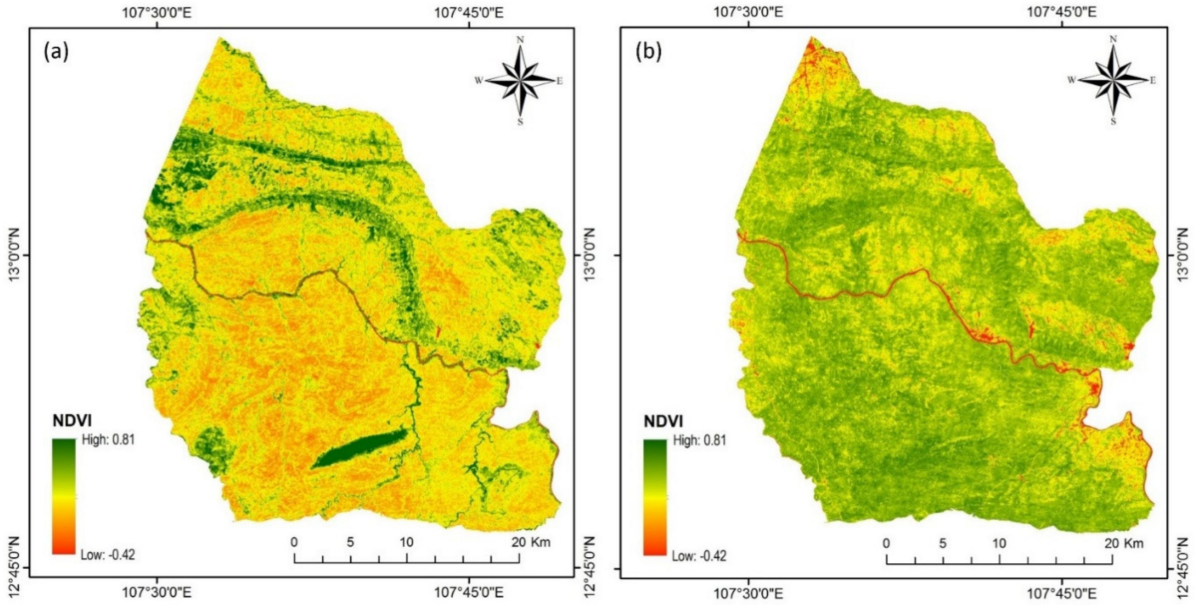

Figure 4. Normalized difference vegetation index (NDVI) images generated from Landsat 8 cloud-free composite images: (**a**) NDVI image in the dry season and (**b**) NDVI image in the rainy season.

NDVI is one of the widely used indices for image classification, monitoring, and rapid assessment of forest quality [5,10,18,20,21,28]. The highest NDVI values correspond to dense vegetation, such as evergreen forests, deciduous trees in the rainy season, or crops at their peak growth stage. Based on the characteristics of the growth, deciduous forest and evergreen forest can be extracted by the difference in NDVI values between the dry and rainy seasons.

Figure 4 shows NDVI values significantly vary between two phenology periods. In the study area, the dry season starts in November and ends in April of the next year, while the rainy season starts in May and ends in October. The time of significant leaf regeneration is from June to October of the year. The NDVI image can discriminate between evergreen and semi-evergreen forests in the dry season because the NDVI values of evergreen forests are much higher than those of the BDFs and the other vegetation types. Evergreen and

semi-evergreen forests are typically distributed in the mountains, on steep slopes, and next to streams or rivers crossing the national park. However, BDFs can be easily mixed with barren land, shrubs, and dried water surface. Thus, it is infeasible to classify them even if only the NDVI image in the dry season is used. On the other hand, NDVI values of vegetation in the rainy season are significantly high and can be easily identified from the other land cover types, such as water and other bare lands. Nevertheless, it is challenging to discriminate between evergreen forests and semi-evergreen forests with BDFs because all types of vegetation in this season grow healthy. Therefore, the combination of NDVIs in the dry and rainy seasons is proposed to resolve the difficulties. Then, the evergreen and semi-evergreen forests, BDFs, and water can be classified by optical images.

3.3.2. Determining the Dominant Species of Broadleaf Deciduous Forest Using Multitemporal SAR Images

The dominant species of DBFs were defined on Sentinel-1A color composite image (where red = images acquired on 17 May 2015, green = images acquired on 30 March 2015, blue = images acquired on 22 February 2015), as shown in Figure 5. February and March is the timeframe for BDF leaves falling, while May is the time for them to revive. The difference in leaf cover of the dominant species during this time period led to the change in the backscatter values on SAR images and the color of the composite image. Analysis of unchanged areas indicates that the combination color is white or black, corresponding to semi-evergreen or evergreen forest and water. Semi-evergreen or evergreen forest is mainly distributed in high mountains or near the Srepok River. In contrast, the locations of deciduous forests are colorful. Figure 5 shows the main dominant species in Yok Don, which appear in different colors on the composite image.

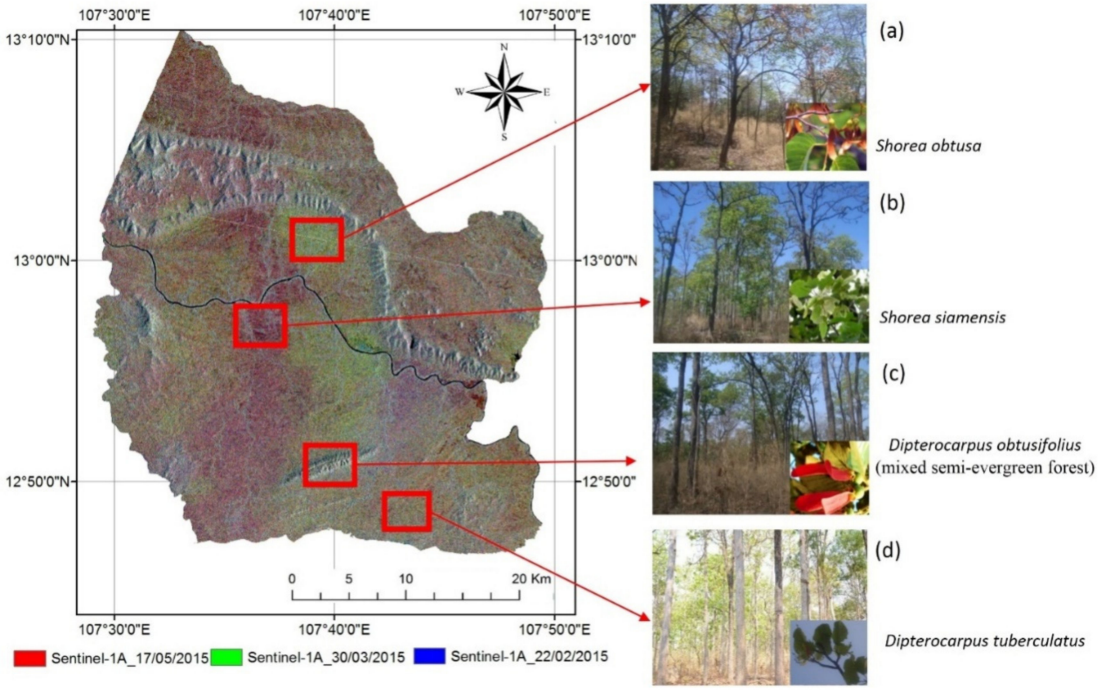

Figure 5. Analysis of deciduous forest species in the composite image: (**a**) *Shorea siamensis*, (**b**) *Shorea obtusa*, (**c**) *semi-evergreen/evergreen*, and (**d**) *Dipterocarpus tuberculatus.*

Backscatter values correspond to the growth process at appropriate locations of the deciduous species on multitemporal SAR images, as shown in Figure 6. It can be clearly seen that Figure 6a–c show the low peak backscattering values in the interval of Date of the Year (DOY) 233 (Day Of the Year of the Julian calendar), the middle of August, and the heaviest rainy time of the year, while Figure 6f,g exhibit the differences in standard deviation and average backscatter values of BDF and semi-evergreen forest. The standard

deviation of semi-evergreen was lower than that of BDF species because there was no change in the backscatter value of semi-evergreen in the period. As a result, the color in the composite multitemporal SAR images of the semi-evergreen area is gray (Figure 6c). In contrast, standard deviations of BDF species were higher, and the average values were lower than semi-evergreen because backscatter signals in SAR image depend on the phenology of trees, ground moisture, and stand structure.

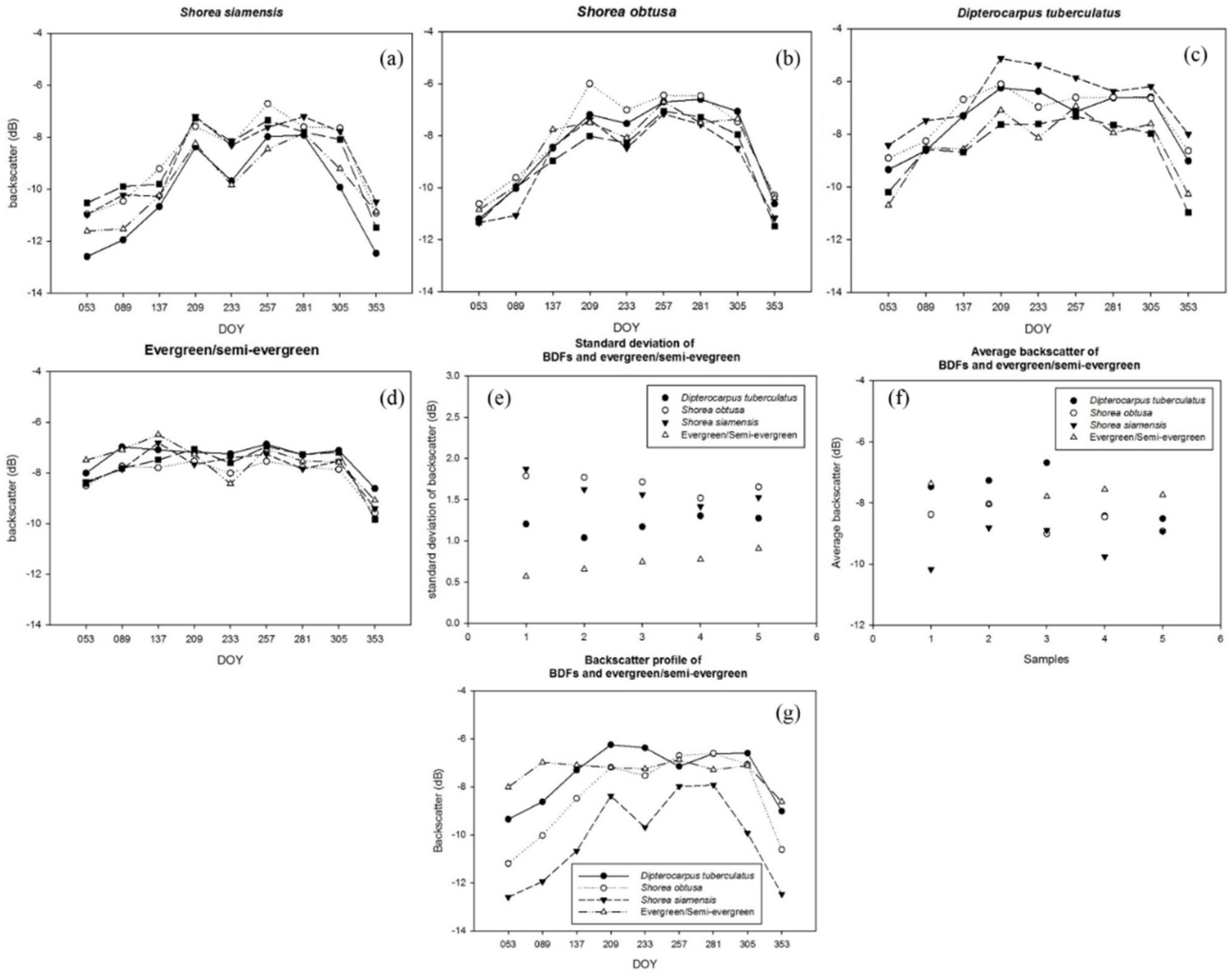

Figure 6. Backscatter profiles of BDFs on multitemporal Sentinel-1A images: (**a**) *Shorea siamensis*, (**b**) *Shorea obtusa*, (**c**) *Dipterocarpus tuberculatus*, (**d**) *evergreen/semi-evergreen*, (**e**) standard deviation backscatter value of BDFs and evergreen/semi-evergreen, (**f**) average backscatter value of BDFs and evergreen/semi-evergreen, and (**g**) comparison of backscatter profile of BDFs and evergreen. DOY (Day of the Year of the Julian calendar).

Semi-evergreen forest and deciduous forest can be interpreted by standard deviation and composite RGB of multitemporal Sentinel-1A images. Features of BDF species were classified based on the field surveying data and the correlation between backscatter values of BDF patterns on multitemporal SAR images and the phenology of deciduous species in Yok Don National Park within the deciduous forest classified area. Because of elevation in this area, *Dipterocarpus obtusifolius* is mixed with semi-evergreen or evergreen. BDF1, BDF2, and BDF3 are assigned as *Shorea siamensis*, *Shorea obtusa*, and *Dipterocarpus tuberculatus*, respectively. Figure 6g shows the growth of deciduous species with the low peaks of backscatter values in fall leaves in February, March, and December because flora status at this time is mainly grass and shrubs. May and July are the times of deciduous tree leaves to bud, with leaves reaching a peak in September. Accordingly, the backscatter signal increases in May and reaches its peak in July to September.

In Figure 6g, *S. siamensis* has the lowest backscatter value compared with the other deciduous species because *S. siamensis* grows in dry land and sparse shrubs. *S. obtusa* has a similar phenology with *S. siamensis*, as shown in Figure 6g. Nevertheless, average backscatter values were higher for *S. obtusa* than *S. siamensis*. As a result, the mean backscatter value in May was a condition to distinguish *S. siamensis* and *S. obtusa*. Figure 6c shows that *D. tuberculatus* is heterogeneous with many differences among plant species. *D. tuberculatus*, which distributes near the bottom of the mountains, has a high density so that the backscatter values are higher than those of the others. Therefore, *D. tuberculatus* was classified by average backscatter values of February and March (Figure 6g).

3.3.3. Proposed Method

Based on the difference in NDVI values between dry and rainy seasons and the correlation between backscatter values of multitemporal SAR images and family *Dipterocarpaceae* growth, we propose an object-based classification scheme as shown in the flowchart given in Figure 7.

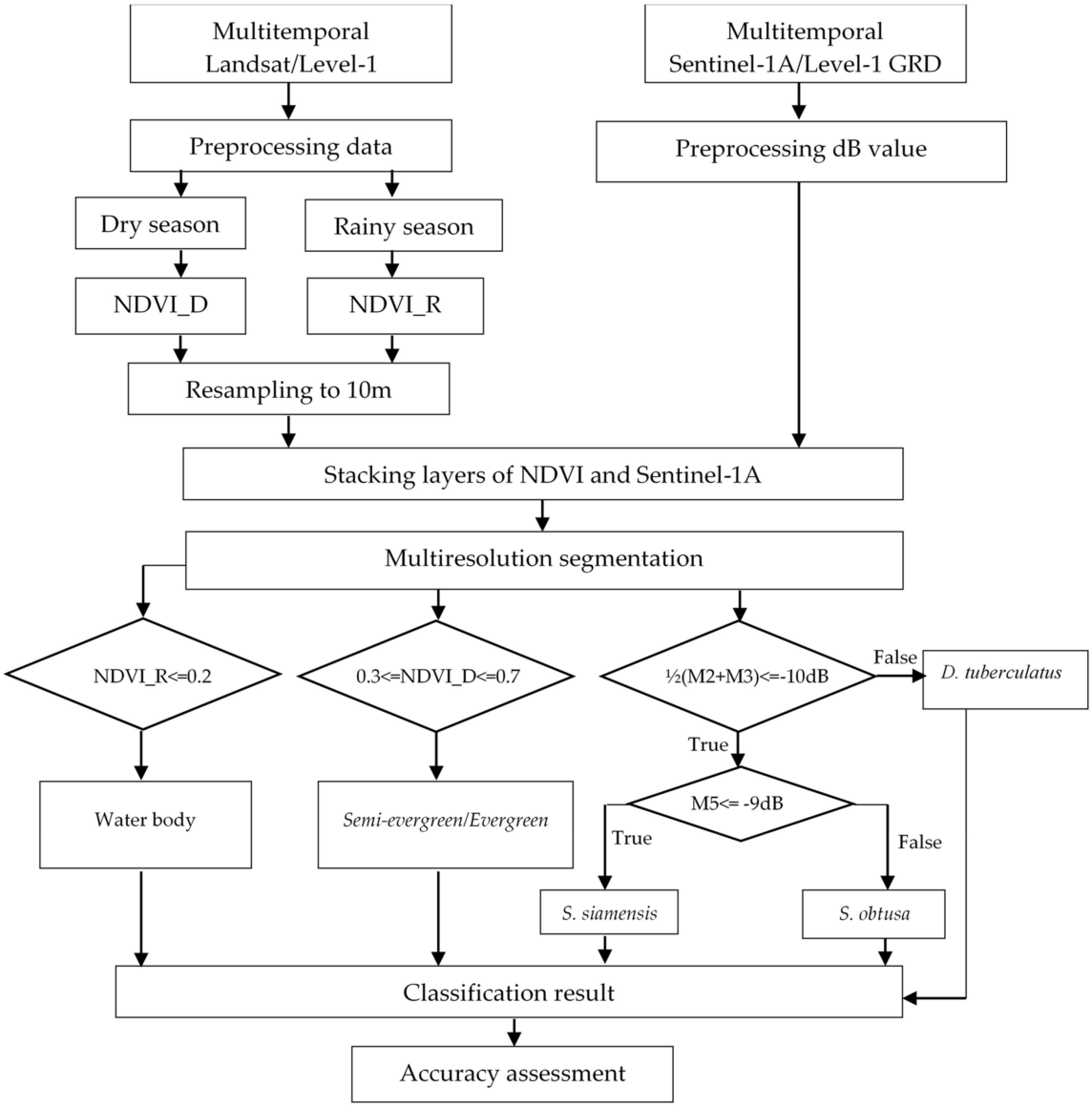

Figure 7. Identification scheme of deciduous forest species by using Sentinel-1A and Landsat 8 images. NDVI_D is the NDVI in the dry season and NDVI_R is NDVI in the rainy season. In this flowchart, M2 is the mean backscatter value in February, M3 in March, and M5 in May.

The classification process was conducted through two main steps: (i) segmentation of 11 bands (including two bands of NDVI images and nine bands of Sentinel-1A images) to define the homogenous objects based on their spectral properties, and (ii) using the threshold of mean values of each homogeneous pattern to classify each object.

First, we tried to identify homogeneous patterns using multiresolution segmentation algorithms based on NDVI images and time-series Sentinel-1A images. Numerous experiments were conducted with different segmentation parameters in the multiresolution segmentation algorithm: (i) keep the same weight of all bands, (ii) scale the parameter to be 10 corresponding to the 10 m spatial resolution of the experimental materials, (iii) change the shape and compactness parameters. Numerous scripts were applied to determine the parameters of the multiresolution segmentation algorithm. Results were compared with reference data and expert knowledge. Final parameters of the multiresolution segmentation algorithm were selected: scale parameter, 10; shape, 0.4; compactness, 0.8; and the same weighted image channels. The homogeneous pattern's segmentation is shown in Figure 8.

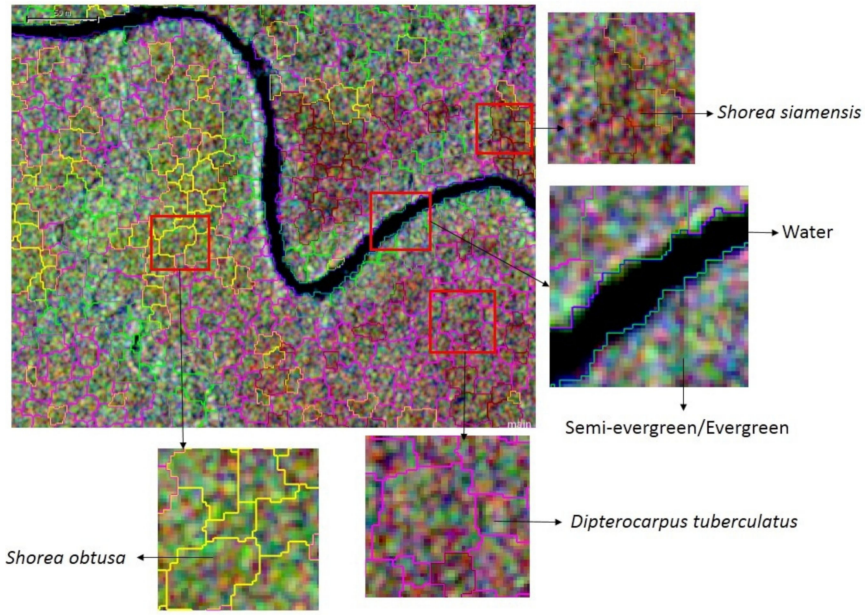

Figure 8. Multiresolution segmentation applied for NDVI (rainy and dry seasons) and multitemporal Sentinel-1A data with parameters: scale, 10; shape, 0.4; compactness, 0.8.

Water, semi-evergreen forest, and evergreen forest were classified by comparison of NDVI values for both dry and rainy seasons. BDFs were classified by the differences between average of backscatter values of multitemporal Sentinel-1A images in February, March, and May. February and March have extremely dry weather and are the time of family Dipterocarpaceae leaves falling. May is the time of regeneration of the family Dipterocarpaceae. It can be seen from Figure 6a–c from July onwards that the BDF leaves strongly regenerate, and the BDFs in this time look like evergreen forests because of higher backscatter values of BDFs, which are similar to backscatter values of evergreen forests. Therefore, we choose the three most typical moments of deciduous trees, including the time of entirely deciduous (February and March) and when the trees start to regenerate leaves (May) to distinguish the three dominant BDF species. The threshold values are shown in Figure 7.

Broadleaf deciduous forests in Yok Don are also known as Dipterocarpaceae family by low density. Their canopies do not intersect. During the dry season, the leaf falling duration of BDF species lasts from 2 to 4 months. The density of trees is about 260–1100 per ha with a diameter of 20 cm. It usually has only one wood canopy with a height from 7 to 25 m. The carpet is not dense. Characteristics of some dominant species in the national park are given in Appendix A.

4. Result and Discussion

4.1. Broadleaf Deciduous Forest Map

Figure 9 shows the classification result and statistics of some BDF types in Yok Don National Park. The spatial distribution of deciduous forest consists of 24% (of the national park's total area) *S. obtusa*, 45% *D. tuberculatus*, 17% *S. siamensis*, 13% *semi-evergreen/evergreen*, and 1% water.

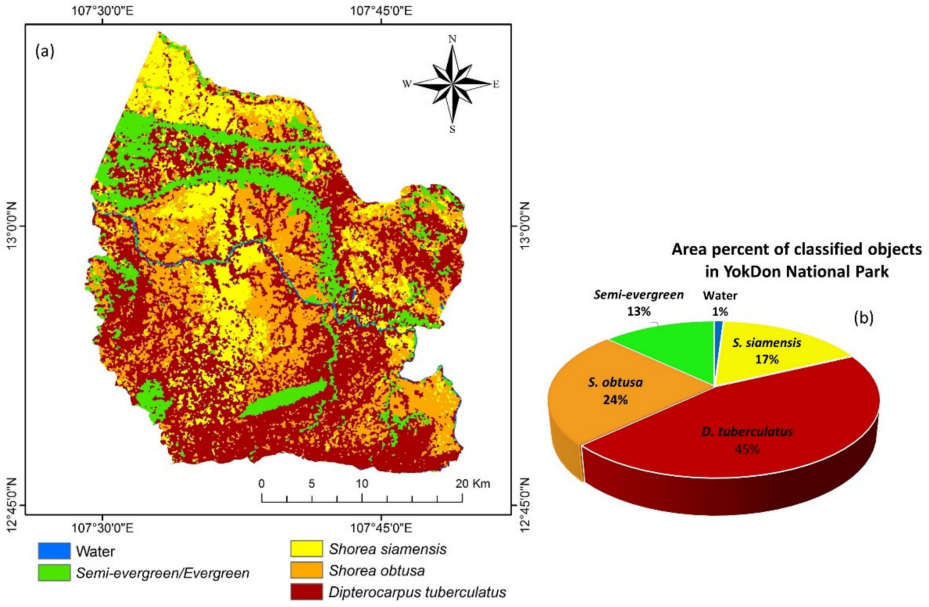

Figure 9. (**a**) Map of BDFs and (**b**) pie chart of area percentage for the classified objects in Yok Don National Park.

4.2. Accuracy Assessment

Accuracy assessment was performed by comparing the classified BDFs with statistical BDFs from the checking plots of field surveying data. In the study area, the dominant deciduous species, such as *S. obtusa, D. tuberculatus,* and *S. siamensis*, were analyzed in the sample plots. We used 66 field survey plots to evaluate the classification accuracy results. The location of the validation points and field photos are shown in Figure 10. Among the 66 validation points, there were 8 semi-evergreen/evergreen plots, 7 *S. siamensis* plots, 23 *S. obtusa* plots, and 28 *D. tuberculatus* plots.

A confusion matrix of broadleaf deciduous forest classification with the user accuracy and producer accuracy per class is shown in Table 3. Results show that 14 plots are misclassified, accounting for 21%. *S. obtusa* has the most misclassification points with seven points. These misclassifications often have many broadleaf deciduous species in a plot with *RBA* values of 50% to 60%. The overall accuracy of the classification is 79% with a kappa coefficient of 0.7.

Table 3. Accuracy assessment of the proposed method.

	Field Surveying Data					
Classes	***Semi-Evergreen /Evergreen***	***S. siamensis***	***S. obtusa***	***D. tuberculatus***	**Total**	**User Accuracy (%)**
Semi-evergreen /Evergreen	7	0	1	2	10	70.0%
S. siamensis	0	7	1	1	9	77.8%
S. obtusa	0	0	16	3	19	84.2%
D. tuberculatus	1	0	5	22	28	78.6%
Total	8	7	23	28	66	
Producer Accuracy %	87.5%	100%	69.6%	78.6%		

Overall accuracy: 78.8%; kappa: 0.7.

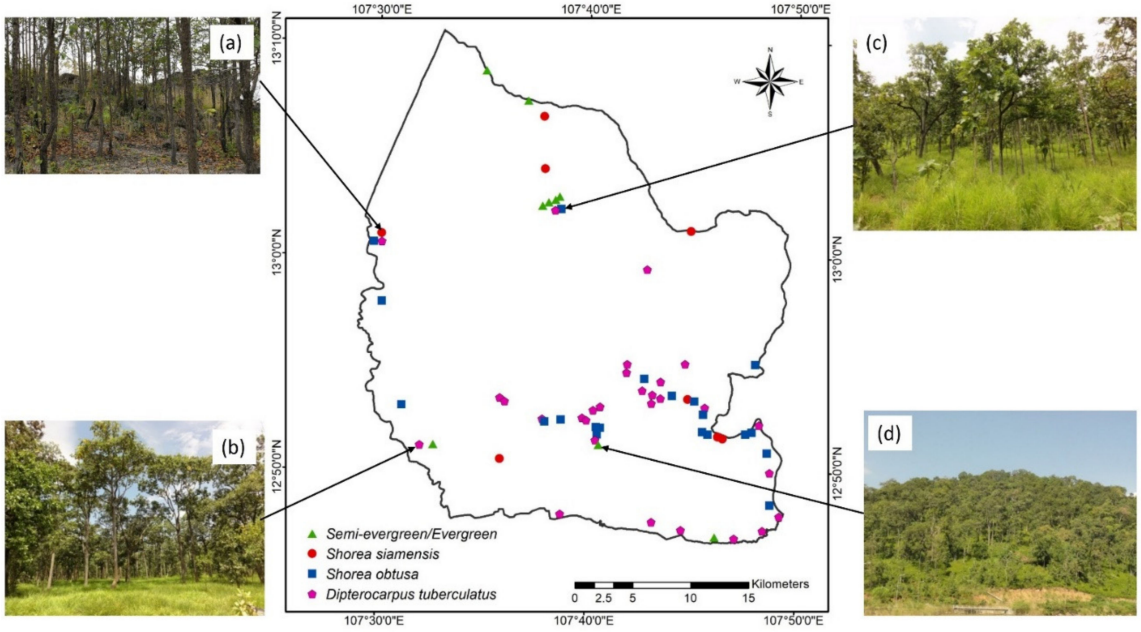

Figure 10. Location of 66 field survey plots for validation and field photos: (**a**) *Shorea siamensis*, (**b**) *Shorea obtusa*, (**c**) *Dipterocarpus tuberculatus*, and (**d**) semi-evergreen/evergreen forest.

4.3. Discussion

We utilized different techniques, including Google Earth Engine, optical imagery, and SAR imagery to derive seasonal composite NDVI imagery. An object-based classification method was applied for the BDF classification. The Landsat images were used to classify broadleaf deciduous forests (BDFs), semi-evergreen/evergreen forest, and water. Optical images are affected by clouds, resulting in infeasibility of generating monthly composite images to observe seasonal variation in phenology. Therefore, multitemporal radar Sentinel-1A images were employed to resolve this problem. Conversely, using radar images alone will face difficulties, such as speckle noise and foreshortening, layover, and shadow distortion in mountainous areas. Thus, the combined optical and radar images effectively improve broadleaf deciduous forest classification in the study area.

The proposed method was the combination of optical and SAR images for BDF classification. It took advantage of the two types of images. The relation of backscattering profiles from time-series SAR images and phenological features of the broadleaf deciduous forest provides us more detailed information about dominant species composition and its evolution. However, foreshortening and layover on a radar image cause misclassification with semi-evergreen/evergreen forests in the mountainous areas. The semi-evergreen/evergreen forest is usually distributed in the high mountain belts and near a water source. In addition, the wetland in the study area changed in the dry season. Hence, Landsat 8 data were used to classify water and semi-evergreen/evergreen forest.

NDVI images of dry and rainy seasons were resampled to 10 m resolution to be integrated with Sentinel-1A images and compared with sample plots (size 20 m $\times$ 20 m). The combination of optical images and multitemporal SAR image was used as input data for the object-based classification method's multiresolution segmentation algorithm to create the segmented homogeneous patterns. Each dominant species has a different time of leaves falling and this characteristic corresponds to backscatter signals. The broadleaf deciduous forest species were identified by taking an average value of segments in each Sentinel-1A image in February, March, and May. The relation of backscatter values of multitemporal Sentinel-1A images and the growth of BDFs were analyzed. The semi-evergreen forest has stable intensity and low standard deviation values, while the dominant species of

BDFs have much fluctuation between the dry and rainy seasons. Backscatter values in the interval of DOY 233 (middle of August—the heaviest rainy time of the year) are lower than those in July and September, likely because the BDFs exhibit healthy growth in this period. Backscattering values derived from the SAR images are influenced by humidity and heavy rain.

The accuracy of classification significantly depends on the homogeneity of deciduous species in the checking plots. Classification results were compared with the BDFs in field surveying data with the assumption of homogeneous species at the checking plots. It is necessary to examine the homogeneous level in the plot sites. Thus, we were able to determine the homogeneous level of BDF species by about 70% in the checking plots. The misclassification only appeared in checking plots with numerous BDF species, and the homogeneous level is less than 50%. Besides, there are exceptional mixed classes. Table 3 shows that the highest accuracy is 84.2% for *S. obtusa* and the lowest accuracy is about 70.0% for semi-evergreen/evergreen forest because of mixed deciduous forests. Based on the field survey data, *S. obtusa* and *D. tuberculatus* are the major BDF species in Yok Don National Park.

This study has further demonstrated that time-series Sentinel-1A imagery can classify deciduous forest species in tropical regions. It indicates a definite relationship between backscattering on Sentinel-1A images and the phenology of deciduous forest species. Marius et al. [9] proved that use of time-series Sentinel-1A images is able to classify deciduous and coniferous forests in northern Switzerland with an accuracy of 86% and kappa coefficient of 0.73. Overall accuracy for individual vegetation species in the study area was 72% with a kappa coefficient of 0.58. Notably, the forest features in northern Switzerland are more homogeneous (80%) compared with that in a tropical forest (homogeneity in our study area is about 50%), which has many layers with the mutual intersection, resulting in misclassification. Thus, it is of more challenge to obtain very high accuracy in forest classification in the tropical region in a deciduous forest. In addition, as far as we know, there is no study in Vietnam using Sentinel-1A for dry dipterocarp forest classification; for other countries in Asia, we searched and found limited references on this same issue.

Our study contributes to enriching the guidance and materials for forest management in Vietnam, which have never been found in the literature since only limited traditional inventory data are currently used [41–44]. Our classification map of deciduous forest in Dak Lak, Central Highlands of Vietnam, and the proposed classification scheme using Sentinel-1A imagery can be applied to the other regions of interest to achieve reliable information and reduce the human workforce.

5. Conclusions

Forest phenology observation and classification is commonly viewed as a vital diagnostic of climate variation, and it is also the first-order control on biosphere–atmosphere interaction. Consequently, Earth observation data have been instrumental in monitoring and mapping the forest phenology over the past decades. Since most efforts are attempted on single data or at larger scales, local-scale investigations with tropical forests are still rare. In this paper, we proposed integrating the multitemporal Sentinel-1A and Landsat 8 images using object-based classification methods to classify the broadleaf deciduous forests with the aid of Google Earth Engine. Then, dominant species in Yok Don National Park can be identified and used for improved management and conservation of the deciduous forest ecosystem in the Central Highlands, Vietnam.

In summary, three key points can be concluded: (i) Experimental results show that reliable classification between water, deciduous forest, and nondeciduous forest can be achieved by using NDVI images of dry and rainy seasons, based on multitemporal SAR images classified for BDF species based on backscatter values. (ii) The proposed method results are compared with field survey data, showing a 79% overall accuracy. (iii) The accuracy of the proposed classification method depends on the level of homogeneity of the species in the study area with the representaive species in the checking plots. We rely

on NDVI and backscattering values derived from time-series optical and SAR images, respectively, to enhance the accuracy of forest species identification in the tropical region. However, to best utilize the available data and further advance the classification schemes, some aspects of efforts should be considered or implemented in the future studies, such as using Sentinel-2 data and analysis of the texture, assessment of canopy water availability [45], calculation the mean spectral band values, and utilization of principal component analysis or machine learning methods, together with the acquisition of knowledge about the vegetation's biophysical characteristics, such as tree height, tree density, and biomass.

Author Contributions: A.T.T. developed the research idea through discussion with M.H.L. A.T.T. prepared the first draft of the manuscript. K.A.N. rewrote, enriched the content, and reconstructed the manuscript. D.D.N. provided comments to A.T.T. A.T.T. and V.T.V. conducted the field survey and collected data. Y.A.L. and K.A.N. significantly improved and finalized the manuscript. All authors have read and agreed to the published version of the manuscript.

Funding: The authors appreciate the support of Tay Nguyen program 2016–2020 with project code, TN18/T10 and MOST of Taiwan with project codes 108-2111-M-008 -036 -MY2 and 108-2923-M-008 -002 -MY3.

Institutional Review Board Statement: Not applicable.

Informed Consent Statement: Not applicable.

Acknowledgments: Satellite data are supported by United States Geological Survey (USGS) and the European Space Agency (ESA). We would like to thank to Nguyen Viet Luong for sharing additional field survey data to cross check our results.

Conflicts of Interest: The authors declare no conflict of interest.

Appendix A

a. *Dipterocarpus tuberculatus*

Dipterocarpus tuberculatus distribute at elevations from 150 to 250 m above sea level, on the ancient alluvium plain or low mountain foot and poor land, and shallow soil (Figure A1). It is rare for them to occur at the top or the ridge of a mountain. It has simple species composition in which the species of Dipterocarpaceae family and *Lagerstroemia* spp. family have the most numbers of individuals. Three common species that are mixed with *Dipterocarpus tuberculatus* are *Terminalia, Shorea siamensis, and Shorea obtusa*. This type of forest has a simple hierarchical structure with a one-floor woody canopy and carpet of fresh bushes and shrubs.

b. *Shorea siamensis*

Shorea siamensis distribute at elevations of 150–200 m above sea level, on dry land, low hills, slopes below 25 degrees, and shallow soil (Figure A2). *Shorea siamensis* usually grow mixed with two common species, *Dipterocarpus tuberculatus* and *Pterocarpus macrocarpus*, and some other species such as *Xylia xylocarpa, Canarium,* and *Aporosa villos,* which are involved in the tree floor and form the stand. In terms of population, there are 95% deciduous individuals with a simple hierarchical structure. This dominant composition has a strong regenerative ability, especially *Shorea siamensis*.

c. *Shorea obtuse*

Shorea obtuse is characterized by its distribution characteristics and formation conditions, similar to those of *Shorea siamensis* (Figure A3). Therefore, these two dominant compositions are often interleaved and set up as simple flora species. *Shorea obtusa* predominates, with up to 50% of individuals and 55% of the total cross-sectional population. This forest type has a simple structure and strong regenerative ability. *Shorea obtusa* is a large timber tree with 25–35-m height, 90-cm in diameter, drought tolerance, and forest fire resistance.

d. *Dipterocarpus obtusifolius*

Dipterocarpus obtusifolius distribute at elevations from 200 to 400 m above sea level (Figure A4). The component of forest species is more complicated because of higher distributional height than those of the others. *Dipterocarpus obtusifolius* is mixed with semi-evergreen or evergreen in more elevated positions.

Figure A1. *Dipterocarpus tuberculatus*.

Figure A2. *Shorea siamensis*.

Figure A3. *Shorea obtuse*.

Figure A4. *Dipterocarpus obtusifolius* (mixed semi-evergreen forest).

References

1. Meyfroidt, P.; Lambin, E.F. Forest transition in Vietnam and its environmental impacts. *Glob. Chang. Biol.* **2008**, *14*, 1319–1336. [CrossRef]
2. Nguyen, K.A.; Liou, Y.A. Global mapping of eco-environmental vulnerability from human and nature disturbances. *Sci. Total. Environ.* **2019**, *664*, 995–1004. [CrossRef]
3. Nguyen, K.A.; Liou, Y.A.; Li, M.L.; Tran, T.A. Zoning eco-environmental vulnerability for environmental management and protection. *Ecol. Indic.* **2016**, *69*, 100–117. [CrossRef]
4. Cleland, E.E.; Chuine, I.; Menzel, A.; Mooney, H.A.; Schwartz, M.D. Shifting plant phenology in response to global change. *Trends Ecol. Evol.* **2007**, *22*, 357–365. [CrossRef] [PubMed]
5. Menzel, A.; Sparks, T.H.; Estrella, N.; Koch, E.; Aasa, A.; Ahas, R.; Alm-Kübler, K.; Bissolli, P.; Braslavská, O.; Briede, A.; et al. European phenological response to climate change matches the warming pattern. *Glob. Chang. Biol.* **2006**, *12*, 1969–1976. [CrossRef]
6. Zhou, L.; Tucker, C.J.; Kaufmann, R.K.; Slayback, D.; Shabanov, N.V.; Myneni, R.B. Variations in northern vegetation activity inferred from satellite data of vegetation index during 1981 to 1999. *J. Geophys. Res.* **2001**, *106*, 20069–20083. [CrossRef]
7. Liou, Y.A.; Nguyen, K.A.; Li, M.H. Assessing spatiotemporal eco-environmental vulnerability by Landsat data. *Ecol. Indic.* **2017**, *80*, 52–65. [CrossRef]
8. Jin, S.; Sader, S.A. MODIS time-series imagery for forest disturbance detection and quantification of patch size effects. *Remote Sens. Environ.* **2005**, *99*, 462–470. [CrossRef]
9. Hansen, M.C.; Potapov, P.V.; Moore, R.; Hancher, M.; Turubanova, S.A.; Tyukavina, A.; Thau, D.; Stehman, S.V.; Goetz, S.J.; Loveland, T.R.; et al. High-Resolution Global Maps of 21st-Century forest cover change. *Science* **2013**, *342*, 850–853. [CrossRef] [PubMed]
10. Hufkens, K.; A Friedl, M.; Sonnentag, O.; Braswell, B.H.; Milliman, T.; Richardson, A.D. Linking near-surface and satellite remote sensing measurements of deciduous broadleaf forest phenology. *Remote Sens. Environ.* **2011**, *117*, 307–321. [CrossRef]
11. Justice, C.; Townshend, J.; Vermote, E.; Masuoka, E.; Wolfe, R.; Saleous, N.; Roy, D.; Morisette, J. An overview of MODIS Land data processing and product status. *Remote Sens. Environ.* **2002**, *83*, 3–15. [CrossRef]
12. Hansen, M.C.; Stehman, S.V.; Potapov, P.V. Quantification of global gross forest cover loss. *Proc. Natl. Acad. Sci. USA* **2010**, *107*, 8650–8655. [CrossRef]
13. Mather, A.S.; Needle, C.L. The forest transition: A theoretical basis. *Area* **1997**, *30*, 117–124. [CrossRef]
14. Nguyen, K.A.; Liou, Y.A. Mapping global eco-environment vulnerability due to human and nature disturbances. *MethodsX* **2019**, *6*, 862–875. [CrossRef] [PubMed]
15. Nguyen, K.A.; Liou, Y.A.; Terry, J.P. Vulnerability of Vietnam to typhoons: A spatial assessment based on hazards, exposure and adaptive capacity. *Sci. Total. Environ.* **2019**, *682*, 31–46. [CrossRef] [PubMed]
16. Nguyen, T.H.; Liou, Y.A.; Nguyen, K.A.; Sharma, R.C.; Tran, D.P.; Liou, C.L.; Cham, D.D. Assessing the Effects of Land-Use Types in Surface Urban Heat Islands for Developing Comfortable Living in Hanoi City. *Remote Sens.* **2018**, *10*, 1965. [CrossRef]
17. Rudel, T.K.; Coomes, O.T.; Moran, E.; Achard, F.; Angelsen, A.; Xu, J.; Lambin, E. Forest transitions: Towards a global understanding of land use change. *Glob. Environ. Chang.* **2004**, *15*, 23–31. [CrossRef]
18. Chen, X.; Vierling, L.; Deering, D.; Conley, A. Monitoring boreal forest leaf area index across a Siberian burn chronosequence: A MODIS validation study. *Int. J. Remote Sens.* **2005**, *26*, 5433–5451. [CrossRef]
19. Coops, N.C.; Wulder, M.A.; Iwanicka, D. Large area monitoring with a MODIS-based Disturbance Index (DI) sensitive to annual and seasonal variations. *Remote Sens. Environ.* **2009**, *113*, 1250–1261. [CrossRef]
20. Forzieri, G.; Castelli, F.; Vivoni, E.R. A predictive multidimensional model for vegetation anomalies derived from remote-sensing observations. *IEEE Trans. Geosci. Remote Sens.* **2010**, *48*, 1729–1741. [CrossRef]
21. Xiao, X.; Biradar, C.; Wang, A.; Sheldon, S.; Chen, Y. Recovery of vegetation canopy after severe fire in 2000 at the Black Hills National Forest, South Dakota, USA. *J. Resour. Ecol.* **2011**, *2*, 106–116.
22. Hargrove, W.W.; Spruce, J.P.; Gasser, G.E.; Hoffman, F.M. Toward a national early warning system for forest disturbances using remotely sensed canopy phenology. *Photogramm. Eng. Remote Sens.* **2009**, *75*, 1150–1156.
23. Delbart, N.; le Toan, T.; Kergoat, L.; Fedotova, V. Remote sensing of spring phenology in boreal regions: A free of snow-effect method using NOAA-AVHRR and SPOT-VGT data (1982–2004). *Remote Sens. Environ.* **2006**, *101*, 52–62. [CrossRef]
24. Maignan, F.; Breon, F.M.; Bacour, C.; Demarty, J.; Poirson, A. Interannual vegetation phenology estimates from global AVHRR measurements:Comparison with in situ data and applications. *Remote Sens. Environ.* **2008**, *112*, 496–505. [CrossRef]
25. Immitzer, M.; Vuolo, F.; Atzberger, C. First experience with Sentinel-2 data for crop and tree species classifications in Central Europe. *Remote Sens.* **2016**, *8*, 166. [CrossRef]
26. Vieira, M.A.; Formaggio, A.R.; Rennó, C.D.; Atzberger, C.; Aguiar, D.A.; Mello, M.P. Object Based Image Analysis and Data Mining applied to a remotely sensed Landsat time-series to map sugarcane over large areas. *Remote Sens. Environ.* **2012**, *123*, 553–562. [CrossRef]
27. Marshall, M.; Thenkabail, P.; Biggs, T.; Post, K. Hyperspectral narrowband and multispectral broadband indices for remote sensing of crop evapotranspiration and its components (transpiration and soil evaporation). *Agric. For. Meteorol.* **2015**, *218*, 122–134. [CrossRef]

28. Maschler, J.; Atzberger, C.; Immitzer, M. Individual Tree Crown Segmentation and Classification of 13 Tree Species Using Airborne Hyperspectral Data. *Remote Sens.* **2018**, *10*, 1218. [CrossRef]
29. Marius, R.; Schaepman, E.M.; Small, D. Using multitemporal Sentinel-1 C-band backscatter to monitor phenology and classify deciduous and coniferous forests in Northern Switzerland. *Remote Sens.* **2017**, *10*, 55. [CrossRef]
30. Quegan, S.; Le, T.T.; Yu, J.J.; Ribbes, F.; Floury, N. Multitemporal ERS SAR analysis applied to forest mapping. *IEEE Trans. Geosci. Remote Sens.* **2000**, *38*, 741–753. [CrossRef]
31. Frison, P.L.; Fruneau, B.; Kmiha, S.; Soudani, K.; Dufrêne, E.; Le Toan, T.; Koleck, T.; Villard, L.; Mougin, E.; Rudant, J.P. Potential of Sentinel-1 Data for monitoring temperate mixed forest phenology. *Remote Sens.* **2018**, *10*, 2049. [CrossRef]
32. Dong, J.; Xiao, X.; Chen, B.; Torbick, N.; Jin, C.; Zhang, G.; Biradar, C. Mapping deciduous rubber plantations through integration of PALSAR and multi-temporal Landsat imagery. *Remote Sens. Environ.* **2013**, *134*, 392–402. [CrossRef]
33. Zhou, T.; Pan, J.; Zhang, P.; Wei, S.; Han, T. Mapping Winter Wheat with Multi-Temporal SAR and Optical Images in an Urban Agricultural Region. *Sensors* **2017**, *17*, 1210. [CrossRef]
34. Achard, F.; Eva, H.D.; Stibig, H.J.; Mayaux, P.; Gallego, J.; Richards, T.; Malingreau, J.P. Determination of deforestation rates of the world's humid tropical forests. *Science* **2002**, *297*, 999–1002. [CrossRef] [PubMed]
35. Pham, T.D.; Yoshino, K.; Bui, D.T. Biomass estimation of Sonneratia caseolaris (l.) Engler at a coastal area of Hai Phong city (Vietnam) using ALOS-2 PALSAR imagery and GIS-based multi-layer perceptron neural networks. *GISci. Remote Sens.* **2017**, *54*, 329–353. [CrossRef]
36. Vafaei, S.; Soosani, J.; Adeli, K.; Fadaei, H.; Naghavi, H.; Pham, T.D.; Bui, D.T. Improving Accuracy Estimation of Forest Aboveground Biomass Based on Incorporation of ALOS-2 PALSAR-2 and Sentinel-2A Imagery and Machine Learning: A Case Study of the Hyrcanian Forest Area (Iran). *Remote Sens.* **2018**, *10*, 172. [CrossRef]
37. Clerici, N.; Calderón, C.A.; Posada, J.M. Fusion of Sentinel-1a and Sentinel-2A data for land cover mapping: A case study in the lower Magdalena region, Colombia. *J. Maps* **2017**, *13*, 718–726. [CrossRef]
38. Forest Monitoring Designed for Action. Available online: https://www.globalforestwatch.org (accessed on 10 November 2020).
39. Nguyen, T.T.; Baker, P.J. Structure and composition of deciduous dipterocarp forest in Central Vietnam: Patterns of species dominance and regeneration failure. *Plant Ecol. Divers.* **2016**, *9*, 589–601. [CrossRef]
40. Rastogi, A. Methods in applied ethnobotany. In *Lessons from the Field*; Discussion Paper Series; International Centre for Integrated Mountain Development: Kathmandu, Nepal, 1999.
41. Ho, V.C.; Pham, B.Q. Biodiversity values and conservation management issues in Yok Don National Park. *J. Agric. Rural Dev.* **2006**, *2*, 65–82.
42. Ngo, T.D.; Ho, V.C.; Nguyen, N.T.; Vu, A.T. The vegetation of Yok Don National Park-A special ecosystem in the Central Highlands. *J. Agric. Rural Dev.* **2006**, *2*, 61–64.
43. Dong, X.S. The main flora advantages of dipterocarp forest in Yok Don National Park and some conservation measures. *J. Agric. Rural Dev.* **2006**, *2*, 80–83.
44. Dong, X.S. Some states of dipterocarp forest in Yok Don National Park and conservation measures. *J. Agric. Rural Dev.* **2006**, *1*, 59–70.
45. Liou, Y.A.; Le, M.S.; Chien, H. Normalized Difference Latent Heat Index for Remote Sensing of Land Surface Energy Fluxes. *IEEE Trans. Geosci. Remote Sens.* **2018**, *57*, 1423–1433. [CrossRef]